

Ricci curvature: An economic indicator for market fragility and systemic risk

Romeil S. Sandhu,^{1*} Tryphon T. Georgiou,² Allen R. Tannenbaum¹

2016 © The Authors, some rights reserved; exclusive licensee American Association for the Advancement of Science. Distributed under a Creative Commons Attribution NonCommercial License 4.0 (CC BY-NC). 10.1126/sciadv.1501495

Quantifying the systemic risk and fragility of financial systems is of vital importance in analyzing market efficiency, deciding on portfolio allocation, and containing financial contagions. At a high level, financial systems may be represented as weighted graphs that characterize the complex web of interacting agents and information flow (for example, debt, stock returns, and shareholder ownership). Such a representation often turns out to provide keen insights. We show that fragility is a system-level characteristic of “business-as-usual” market behavior and that financial crashes are invariably preceded by system-level changes in robustness. This was done by leveraging previous work, which suggests that Ricci curvature, a key geometric feature of a given network, is negatively correlated to increases in network fragility. To illustrate this insight, we examine daily returns from a set of stocks comprising the Standard and Poor’s 500 (S&P 500) over a 15-year span to highlight the fact that corresponding changes in Ricci curvature constitute a financial “crash hallmark.” This work lays the foundation of understanding how to design (banking) systems and policy regulations in a manner that can combat financial instabilities exposed during the 2007–2008 crisis.

INTRODUCTION

As a result of the 2007–2008 financial crisis, much attention has been devoted to understanding the fragility of financial systems (1). A recently accepted model is one in which these interconnected systems are represented as weighted graphs whereby the nodes denote an economic agent and the edge links characterize dependencies and correlations among such agents (for example, returns, debt, and derivative exposure) (2–5). In turn, systemic risk (6) can be taken as a network’s inability to handle default of one or more agents, resulting in cascading failures and triggering the onset of a financial contagion; that is, in a given financial network, one must be able to attribute a proper measure of risk to specific institutions (nodes) and, more importantly, to their interrelationships (edges) that are often deemed “too big to fail.” The need for such a conceptual and quantitative indicator is especially evident in the context of the emergency aid that was provided by the U.S. Federal Reserve Bank (FED) during the 2007–2008 crisis (7). As shown in Fig. 1, there is a series of indirect “hidden” exposures that unraveled during this time period. Understanding how to account for these indirect linkages as opposed to direct exposure is at the core of this work. At the same time, quantifying fragility in the context of financial systems may provide not only a measure of preventing (combating) financial contagions but also novel insights into designing downside protection (value-at-risk) measures.

The goal of this paper is to demonstrate that Ricci curvature may serve as a quantitative indicator of the systemic risk in financial networks and the fragility of financial markets. Curvature, in the broad sense, is a measure by which a geometrical object deviates from being flat. Hence, it has been characterized in various ways in Riemannian geometry (8). In the context of networks, “flatness” is to be understood to reflect the connectivity and interdependence between distant nodes. The proper generalization of curvature and of flatness for discrete spaces, such as networks that are modeled as weighted graphs, is a

very recent development (9–13). From this new vantage point, we examine in this study the topology of stock correlation networks constructed from the Standard and Poor’s 500 (S&P 500) over a 15-year span, and we show that curvature is a “crash hallmark” and a possible economic risk indicator. Although the initial analysis herein is restricted to correlation networks, one may naturally apply our analysis to information-based quantities that pertain to the banking ecosystem (2, 3) or more complex financial instruments (14), which can be a subject of future research. On the other hand, we use the evolution of the stock market as a data platform to primarily illustrate an interesting connection between Ricci curvature and a well-established notion of entropy. We now revisit several key papers that are related to the present work.

First, we note that this study is a follow-on and a complementary effort of previous work where we showed that an increase in Ricci curvature is negatively correlated to an increase in system-level fragility. This is expressed as $\Delta Ric \times \Delta F \leq 0$ and was explored in the context of gene regulatory networks with application in differentiating stages of cancer (15), and is revisited in this work for the sake of completeness. We note that recent advancements have also explored the concepts of fragility on weighted graphs (and the construction thereof) (16–19). In particular, Demetrius *et al.* (16, 20) formally defined “robustness” in terms of the rate function from the theory of large deviations and showed that this is positively correlated to entropy using the Fluctuation Theorem. The insight in this connection is to link robustness to the ability of a network to dissipate disturbances. The key difference in our approach is that Ricci curvature serves as a proxy for robustness/fragility at the edge level of any weighted graph as compared to entropy, which is formulated as a nodal attribute; that is, unlike entropy, which, by construction, exhibits “loss of information” due to a weighted contraction of edge dependencies, Ricci curvature preserves such geometric quantities. Similar to the findings of Demetrius *et al.* (16, 20), Ricci curvature quantifies the ability of the network to dissipate locally along edges. It further allows us the freedom to construct various possible nodal measures.

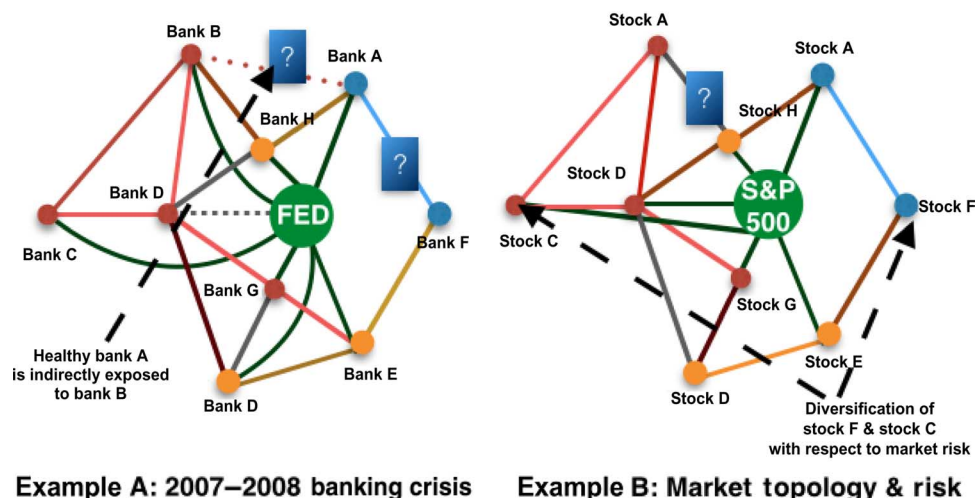
In the context of financial networks, various works seek to examine the fragility of interactions (edges) to better characterize market complexity (2, 14, 21–23) (a complete review is beyond the scope of

¹Departments of Computer Science and Applied Mathematics and Statistics, Stony Brook University, Stony Brook, NY 11794, USA. ²Department of Electrical and Computer Engineering, University of Minnesota, Minneapolis, MN 55455, USA.

*Corresponding author. Email: romeil.sandhu@stonybrook.edu

Measuring local fragility and financial risk exposure

$$\Delta Ric \times \Delta F \leq 0$$



**How can we quantify risk of an economic agent and its relationships?
(that is, debt obligation, derivative exposure, market returns)**

Fig. 1. Systemic risk as a complexity problem: How to account for multiple indirect risk exposures in a financial ecosystem. Understanding indirect counterparty risk has gained increasing importance with the recent global financial crisis combined with the continuous rise of complex financial instruments. This paper proposes a new metric for characterizing instability with respect to agent-to-agent information in the context of a global network, and we illustrate the method by characterizing market fragility from a feedback perspective resulting from well-known “herding” phenomena during periods of financial crisis.

this work, but we highlight several recent studies). Recently, Battiston *et al.* (2) proposed the concept of DebtRank to analyze systemic risk due to debt obligations for general banking environments (3), further expanding on the need to understand the instability of complex derivatives (14) to more tacit areas of corporate control in economic networks (24). The main thrust and motivation in these works is “feedback centrality,” for which we now introduce the concept of Ricci curvature as a feedback measure. With respect to stock correlation networks, Mantegna (4) first illustrates the hierarchical arrangement of stocks through minimum spanning trees (MSTs). This was followed by several works of Onnela *et al.* (5, 25, 26), which leverage the concept of MST to exploit the underlying return dynamics. In particular, the authors show that during crash periods, the tree structure “shrinks and tightens” compared to normal market behavior and those stocks that serve as “leaves” of the tree correlate to diversification with respect to portfolio construction pioneered by Markowitz (27). This study seeks to cast existing work on correlation networks in the context of curvature, fragility, and uncertainty, while also paving the way to analyze more interesting financial networks commonly seen in interbank lending markets that will be considered in future research.

RESULTS

We now present results that link curvature to the fragility of the financial stock market by first providing a definition of robustness, intro-

ducing curvature, and then unifying such concepts through entropy. We then supplement these findings with empirical results that illustrate curvature as a crash hallmark and its relation to entropy, and recast the problem of global minimum variance (GMV) portfolios and leptokurtic distributions commonly used to model asset returns in the context of curvature.

Robustness and fragility

Here, we provide a precise definition of robustness (and, hence, fragility). Given a network, one can consider a random perturbation that results in a deviation of some observable. More formally, let $q_\delta(t)$ denote the probability that the mean deviates by more than δ from the original value at some time t . Under standard assumptions (19, 20), $q_\delta(t) \rightarrow 0$ as $t \rightarrow \infty$, and the relative rate at which the system “relaxes” and returns to its unperturbed state measures its fragility (for example, longer decay rates are analogous to more fragile states) and is given by the following rate function

$$R := \lim_{t \rightarrow \infty} \left(-\frac{1}{t} \log q_\delta(t) \right) \quad (1)$$

Therefore, a large R means a fast return to the original state (robustness), and a small R corresponds to a slow return (fragility). In thermodynamics, it is well known that entropy and rate functions from large deviations are very closely related (19). The Fluctuation

Theorem (19, 20) is an expression of this fact for networks and may be expressed in terms of fragility $\Delta F := -\Delta R$ as

$$\Delta S_e \times \Delta F \leq 0 \tag{2}$$

where S_e denotes network entropy defined in “Details on network entropy” under Materials and Methods.

Revisiting curvature

We now present an intuitive discussion of Ricci and sectional curvature (for formal details, see “Details on Ricci curvature” under Materials and Methods). Accordingly, let X be a Riemannian manifold. One may consider the following surfaces as concrete examples: a sphere, a saddle (hyperbolic paraboloid) surface, and a flat planar surface. Let us denote the vertices of a geodesic triangle on each of the respective surfaces by x_0, x_1, x_2 (Fig. 2). Note that a geodesic triangle is one in which each of its sides is a curve whose length is the shortest distance between the given points. Locally, such geodesic curves exist. Now, let x_m be the midpoint of the geodesic curve connecting points x_0 and x_1 . If X possesses nonnegative sectional curvature (a sphere or a flat planar surface), then the following equation holds for all sufficiently small triangles

$$d(x_2, x_m)^2 \geq \frac{1}{2}d(x_2, x_0)^2 + \frac{1}{2}d(x_2, x_1)^2 - \frac{1}{4}d(x_0, x_1)^2 \tag{3}$$

where d is the distance on X . This inequality illustrates that under positively curved spaces (sphere), triangles are “puffier” than Euclidian triangles (planar surface), as shown in Fig. 2 (A and B). If X has a negative sectional curvature, triangles are “skinnier” than the normal Euclidean counterpart, as depicted in Fig. 2C. By taking the average of sectional curvatures of a Riemannian manifold, one arrives at a Ricci curvature (for further details, see “Details on Ricci curvature” under Materials and Methods).

This said, given that we are working on a graph, one needs an appropriate discrete notion that captures the above behavior. Here, we

used a neat notion of a Ricci curvature, obtained from the work of Ollivier (9, 10, 29). The idea is motivated from the notion that the distance between two small (geodesic) balls is less than the distance between their centers in a positively curved space (and greater than the distance between the centers in a negatively curved one).

In particular, if we let (X, d) be metric space equipped with a family of probability measures $\{\mu_x : x \in X\}$, we define the Ollivier-Ricci curvature $\kappa(x, y)$ along the geodesic connecting nodes x and y via

$$\kappa(x, y) = 1 - \frac{W_1(\mu_x, \mu_y)}{d(x, y)} \tag{4}$$

where W_1 denotes the Wasserstein-1 distance (30–38) and d is the distance on X . This is the discrete analog of the preceding characterization of Ricci curvature. Here, μ_x and μ_y play the role of “geodesic balls”; thus, the distance between “centers” $d(x, y)$ is being compared to the distance between the balls μ_x and μ_y (via the Wasserstein-1 distance). The precise definition of W_1 is given in “Details on Wasserstein distance” under Materials and Methods, and we note that d here is taken to be the “hop” distance on a graph (that is, the shortest path between vertices). For the case of weighted graphs, we set

$$d_x = \sum_y w_{xy} \text{ and } \mu_x(y) := w_{xy}/d_x$$

where d_x is the sum taken over all neighbors of node x and where w_{xy} denotes the weight of an edge connecting node x and node y ($w_{xy} = 0$ if $d(x, y) \geq 2$). A practical example of setting up the problem to compute Ricci curvature on a graph is shown in fig. S1. In addition, the measure μ_x may be regarded as the distribution of a one-step random walk starting from x , with the weight w_{xy} quantifying the strength of interaction between nodal components or the diffusivity across the corresponding link (edge). The Wasserstein-1 distance W_1 may be computed as a linear program that allows for an efficient, highly parallelizable

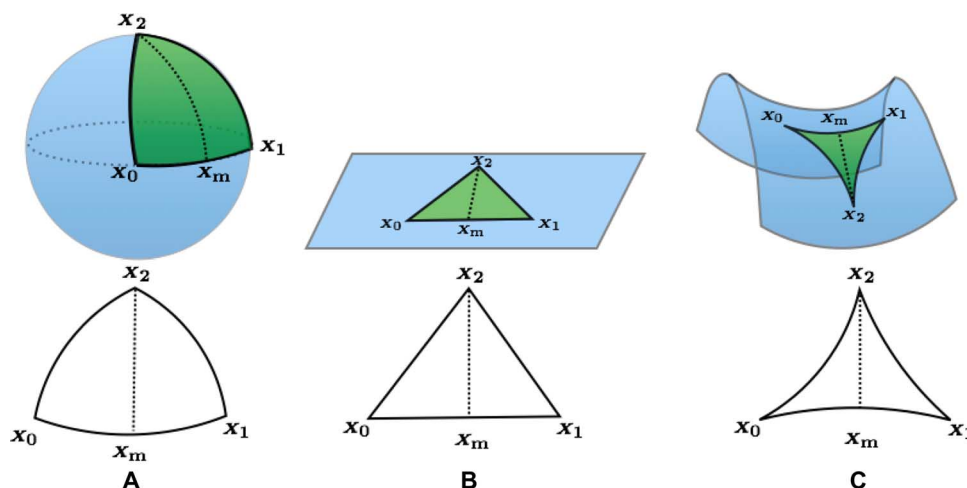


Fig. 2. An intuitive understanding of curvature. (A to C) We compare geodesic triangles, which are triangles in which each side is connected by the shortest (geodesic) curve for three different surfaces: (A) sphere, (B) planar surface, and (C) hyperbolic paraboloid. From the bottom row, we can see that such triangles on a sphere are puffier than their Euclidean planar surface counterparts (due to great circles being geodesics as opposed to straight lines). As we move toward negatively curved space, such triangles become skinnier. This behavior is noted by measuring the length of the (geodesic) curve connecting the midpoint x_m to x_2 .

algorithm (see “Details on Wasserstein distance” under Materials and Methods).

The question of how the curvature discussed above relates to the robustness (and, hence, fragility) of a dynamical system remains. The main ingredient that links these quantities is entropy, which is discussed next.

Entropy, curvature, and fragility

Here, we present a key result from Lott and Villani (11) that shows the deep connection between curvature and entropy. Accordingly, let (X, d, m) denote a geodesic space and set $P(X) := \{\mu \geq 0 : \int_X dm = 1\}$. Then, it can be shown that X has a nonnegative Ricci curvature if and only if for every $\mu_0, \mu_1 \in P(X)$, there exists some geodesic μ_t path with respect to the Wasserstein-2 metric (see Materials and Methods) connecting μ_0 and μ_1 , such that

$$S_e(\mu_t) \geq tS_e(\mu_0) + (1 - t)S_e(\mu_1) \text{ for } 0 \leq t \leq 1 \quad (5)$$

where $S_e := -\mathcal{H}(\mu) = \int \mu \log \mu dm$ is the Boltzmann entropy. To illustrate this concept in an intuitive manner, we revisit the sphere (a positively curved space) for which we would like to “transport” a region defined by a set of points located on the northern hemisphere to its respective region on the southern hemisphere, such that it requires minimal work (shortest path). This is shown in fig. S2. Here, geodesics between any two points are great circles. Moreover, one can see by transporting along these great circles that there is an expansion or “spreading” of this region that encapsulates all individual points being transported. The gist of Eq. 5, as noted by Lott and Villani (11), is that if we consider such points to be gas particles with prescribed initial and final configurations (regions/densities), then entropy is concave along the transport path.

The result of Eq. 5 may be generalized to include arbitrary Ricci curvatures. Indeed, X has a Ricci curvature bounded from below by k if and only if for every $\mu_0, \mu_1 \in P(X)$, there exists some geodesic μ_t path connecting μ_0 and μ_1 , such that

$$S_e(\mu_t) \geq tS_e(\mu_0) + (1 - t)S_e(\mu_1) + \frac{kt(1 - t)}{2} W(\mu_0, \mu_1)^2 \text{ for } 0 \leq t \leq 1 \quad (6)$$

The latter equation indicates that entropy and curvature are positively correlated, which we express as $\Delta S_e \times \Delta Ric \geq 0$. Using the Fluctuation Theorem, we can show that Ricci curvature and fragility are negatively correlated, which we express as $\Delta Ric \times \Delta F \leq 0$. In the next section, we use these findings not only to empirically show that curvature may serve as a “crush hallmark,” but also to show that entropy and curvature are empirically related.

Market fragility and potential applications

This section provides empirical results of financial market fragility using the S&P 500. We note that although more interesting networks exist and recent studies show that correlation networks should be taken with caution in analyzing system risk (39), our motivation here is to introduce the unstudied geometric (curvature) view of markets. In turn, we believe that such work provides an exciting avenue and an alternative perspective to understanding the complex nature of the market.

Network construction. We obtained historical closing daily price data from <https://quantquote.com/>. In particular, the publicly available data set consists of stocks currently comprising the S&P 500 for a 15-year span from January 1998 to July 2013. We then filtered those equities that do not have data for the entire period, resulting in a total of 388 stocks and thereby allowing us to compute the correlation values c_{xy} over a specific time window denoted as T . Then, following Onnela *et al.* (5), we constructed an MST using Prim’s algorithm in MATLAB 2013a where the “distance” is defined to be $\hat{c}_{xy} := \sqrt{2(1 - c_{xy})}$. This was done under the assumption that, at any given time, a particular stock must “interact” with another stock and that the MST provides this basic “skeleton” of the overall market. To examine the topology of the market through a dynamic process, we added high-valued links that satisfy a certain threshold, that is, $c_{xy} \geq \xi$, where we chose $\xi = 0.85$ on the basis of previous literature (40, 41). This can be akin to biological (cancer) network construction in which links are established when two genes have been coexpressed at varying time intervals of a metastatic and/or drug therapeutic study. Moreover, for a given window $t^b = [t_0^b, \dots, t_T^b]$, we constructed an unweighted network \mathcal{N}^b through the above process. A new network at $b + 1$ is generated by “sliding” the window of 1 day and repeating the process. Hence, approximately 4000 time-varying networks are generated.

Market fragility. We computed the Ricci curvature $\kappa(x,y)$ for all possible direct and indirect pairs (approximately 75,000 pairs) over two different time windows, $T = \{22,132\}$ days, for stock correlation networks representing the returns of the S&P 500. These time windows were chosen to represent “short” and “long” time horizons and may be altered (for example, 90 days); longer time windows have the effect of smoothing the resulting data. Nevertheless, Fig. 3 presents the average Ricci curvature.

Figure 3 shows that the market operates in a generally fragile behavior. As noted by a previous study (5), there is a topological market reorganization that occurs during periods of financial crisis. This is partly due to the establishment of more links in crash periods that naturally arise from the well-known herding effect. Constructing correlated graphs in a dynamic manner presents the market from a feedback perspective (by analyzing curvature) as opposed to merely an average correlation between any two given pairs of stocks. Specifically, recent work shows that the lower bound of Ricci curvature characterizes the number of triangles in a graph, and in turn, the number of triangles characterizes the number of differing (redundant) feedback pathways that exist (42). Similar to other man-made systems (for example, aircraft), redundancy is a design characteristic that helps ameliorate the effect of possible random perturbations. Here, in the sense of networks, feedback and curvature are very closely linked. Following this, Fig. 3 illustrates that even with two distinct time scales, there is an increase in Ricci curvature and, thus, the market tends to become more robust during periods of crisis. This is consistent with previous analysis in which Onnela *et al.* (5) examined the shortest average path between equities during such time periods and uncovered that the MST “shrinks.” Again, measuring Ricci curvature on these stock correlation networks illustrates fragile market behavior and the robustness of financial crashes.

Comparison of robustness measures. Although the intended focus of the present work is to study the fragility and robustness of financial (correlation) networks with respect to curvature, it is very important to compare Ricci curvature to other accepted models characterizing network fragility and robustness. To this end, Figs. 4 and 5

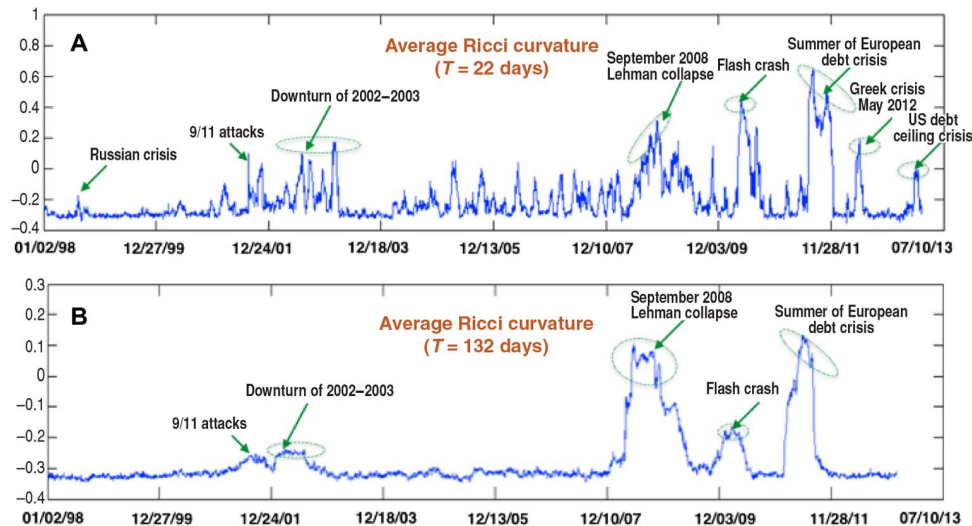


Fig. 3. Average Ricci curvature over a 15-year span of the S&P 500. (A) Choosing a window of $T = 22$ days, we see that curvature captures several financial crashes and show that, on average, market behavior is fragile. **(B)** We extended our analysis with a larger window of $T = 132$ days, and as one can see, there is an increase in Ricci curvature compared to normal fragile market behavior during periods of known financial crisis.

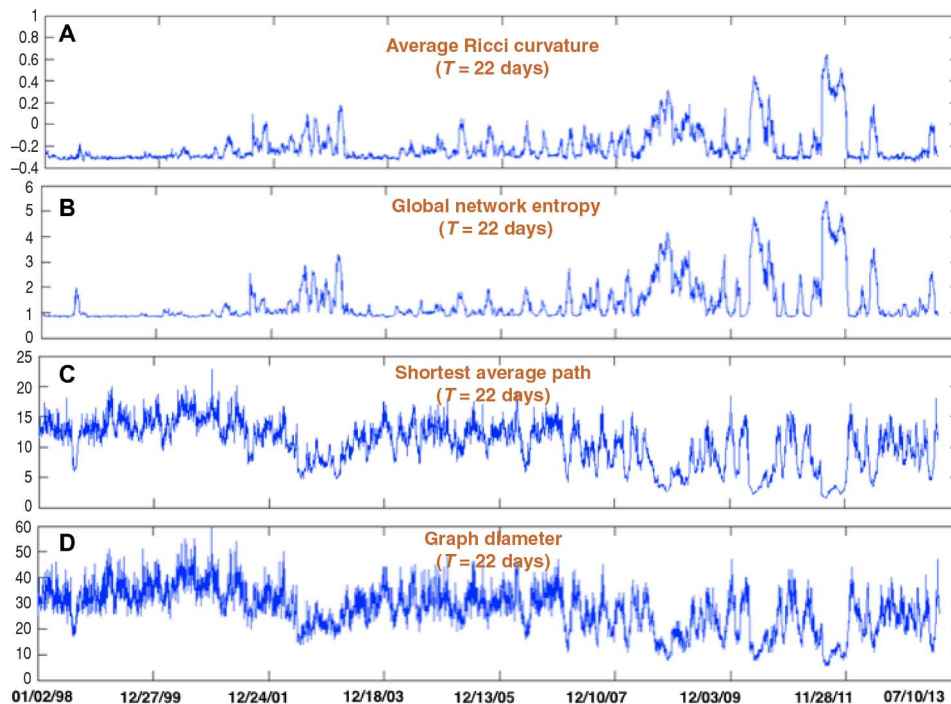


Fig. 4. Comparison of network robustness measures over a smaller time window. (A to D) We compare Ollivier-Ricci curvature (A) to network entropy (B), shortest average path (C), and graph diameter (D) for a shorter time scale of 22 days. As predicted, there is a notable resemblance between network entropy and network curvature. Further analysis shows that decreases in graph diameter and shortest path length result in increases in graph curvature.

plot curvature against global network entropy, shortest average path, and graph diameter. One can see that there is a striking resemblance in the structure of Ricci curvature and global network entropy (see “Details on network entropy” under Materials and Methods for network entropy computation). This is also seen numerically in Table 1. We are uncovering information similar to that about entropy with two

very important caveats: First, the method proposed herein is computationally more tractable and is better behaved than entropy-based techniques; we are simply using an algorithm based on linear programming, which is capable of characterizing curvature between any two nodes in a graph (not only those that are adjacent) to account for possibly significant indirect effects. Second, Ricci curvature provides

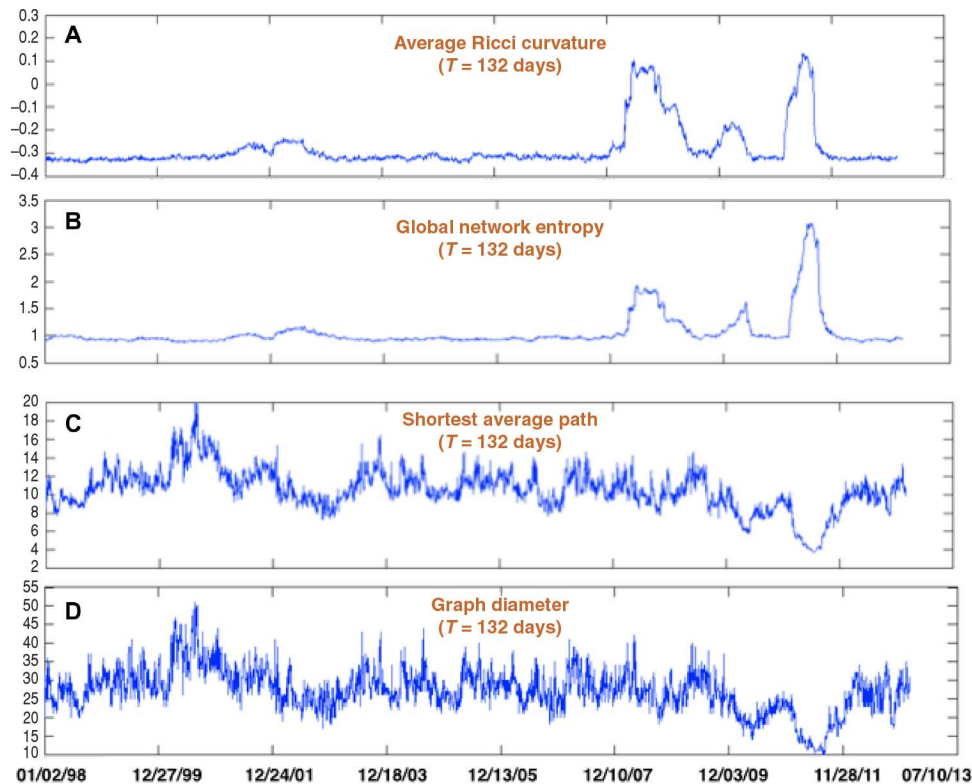


Fig. 5. Comparison of network robustness measures over a larger time window. (A to D) We compare Ollivier-Ricci curvature (A) to network entropy (B), shortest average path (C), and graph diameter (D) for a longer time scale of 132 days. As predicted, there is a notable resemblance between network entropy and network curvature. Further analysis shows that decreases in graph diameter and shortest path length result in increases in graph curvature.

Table 1. Comparison of network robustness measures. We provide the average Ricci curvature, average global network entropy, average shortest path, and average graph diameter computed over a period of 1 year beginning with 1 January of each year with a window $T = 22$ days and a threshold of $\xi = 0.85$. As seen in the graph, a correlation between curvature and well-known measures of fragility.

Measure	Jan 1998	Jan 1999	Jan 2000	Jan 2001	Jan 2002	Jan 2003	Jan 2004	Jan 2005	Jan 2006	Jan 2007	Jan 2008	Jan 2009	Jan 2010	Jan 2011	Jan 2012
Curvature	-0.297	-0.304	-0.285	-0.218	-0.0166	-0.256	-0.253	-0.214	-0.245	-0.218	-0.068	-0.141	-0.101	0.023	-0.0255
Entropy	0.941	0.862	0.909	1.123	1.505	1.193	1.022	1.128	1.066	1.316	2.159	1.745	2.105	2.688	1.282
Shortest path	12.412	13.811	14.910	12.951	9.362	10.199	12.291	11.845	12.413	9.636	7.186	8.060	7.469	6.208	9.545
Diameter	31.361	34.726	38.210	33.186	25.500	27.397	31.250	29.929	31.494	25.064	21.044	22.480	20.964	17.770	25.144

local geometric (edge) information about the network as opposed to entropy, which is a nodal measure. In particular, one can visualize a scenario in a more complex financial network where a particular financial institution generally consists of normal risk exposures to other institutions with only a few extremely (indirect) risky transactions. By averaging such exposures, a nodal measure may not properly address the localized fragility of such relationships. This type of scenario has been shown by studying transcriptional networks of varying cancer tissues wherein a single gene may participate in both robust and fragile interactions, yet is considered a “robust” gene (15). This being said, Figs. 4 and 5 also illustrate that increases in Ricci curvature are correlated with a decrease in shortest average path and graph diameter.

This agrees with previous work on entropy, robustness, and such measures (16) and is reflected in fig. S3.

GMV portfolios. We now shift our focus to the role that curvature and entropy (measures of fragility) may play with respect to the classical Markowitz portfolio construction in the current setting. In the classical case, given a set of N assets with average returns, denoted as $\bar{r} = [\bar{r}_1, \bar{r}_2, \dots, \bar{r}_N]^T$, and the estimated covariance Σ_r (both usually computed from historical data), one is given the task of allocating N asset weights $w = [w_1, w_2, \dots, w_N]^T$ to maximize the portfolio return $u = w^T \bar{r}$, subject to some risk tolerance $w^T \Sigma_r w \leq \tau_{\text{risk}}$ with $\sum_{i=1}^N w_i = 1$ and $w_i \geq 0$ (no short selling). The efficient frontier portfolios (27)

can then be computed for varying levels of risk tolerance; in this case, we are interested in the GMV portfolio. This can be stated as $\min_w w^T \Sigma w$, subject to $\sum_{i=1}^N w_i = 1$ (full investment) and $w_i \geq 0$ (no short selling). To relate risk and curvature, we propose the following measure, which is simply a projection of Markowitz portfolio weights from the minimum risk portfolio onto edge Ricci curvature

$$W_{\text{port}}^{\mathcal{K}} = w^T B w \tag{7}$$

where B denotes the $n \times n$ matrix whose entries are the Ricci curvature between any two given equities [that is, entries are given by $B_{ij} = 1 - W_1(\mu_x, \mu_y)/d(x, y)$ for $1 \leq i, j \leq n$, where μ_x and μ_y are one-step random walks on the graph defined in the “Market fragility and potential applications” section and where $d(x, y)$ is the hop distance]. We note that the above symmetric matrix B is not generally positive definite (and, hence, does not define a metric) but is proposed here to illustrate curvature and its connections to risk. In particular, the weights w for the minimum variance portfolio are computed over a 132-day sliding time window (~6 months) using MATLAB 2013a. Then, for this particular window in which weights were computed, we construct an equivalent correlation network over the same time horizon to compute Ricci curvature between all pairwise stock relationships. Figure 6 shows the measure $W_{\text{port}}^{\mathcal{K}}$ computed in addition to the minimum risk profile. One can see that a correlation exists between an increase in $W_{\text{port}}^{\mathcal{K}}$ and an increase in the minimum risk profile done in classical finance; that is, curvature represents the ability to diversify one’s assets to achieve a minimum risk during varying time periods. Moreover, the above trend seemingly agrees with a previous analysis that points out that diversification “melts away” during periods of crisis (43). This is analogous to increases in curvature that are seen in Figs. 3 and 6, and it will be interesting to compare such existing measures (44) focused on estimating risk. On the other hand, we have previously noted that higher Ricci curvature is also positively correlated to the mean-reverting coefficient in an Ornstein-Uhlenbeck

sense (15). Thus, during times of financial crises where volatility rapidly increases, there are opportunities to construct mean-reverting portfolios (45) commonly used in statistical arbitrage (for example, a perturbation in the portfolio will quickly return to some equilibrium).

Remarks on leptokurtic distributions

Because the thrust of the present work is to introduce curvature as an economic indicator of systemic risk, we revisit the notion of leptokurtic distributions and their connection to Ricci curvature. In particular, it has been argued that stock returns in the market should be modeled as heavy-tailed distributions as opposed to the standard normal distribution (46–48). This is done, in part, to better account for risk management in the event of financial crash and relatable black swan events. Accordingly, let us consider one such leptokurtic distribution, namely, the Laplace distribution with a given mean θ and variance φ and a corresponding normal distribution with the same mean and variance. It is well known that the entropies of Laplacian $S_e^{\mathcal{L}}$ and Gaussian $S_e^{\mathcal{G}}$ distributions are given by the following

$$S_e^{\mathcal{G}} = \frac{1}{2} \log(2\pi e \varphi^2) \tag{8}$$

$$S_e^{\mathcal{L}} = 1 + \log\left(2\sqrt{\frac{\varphi}{2}}\right) \tag{9}$$

Here, we see that $S_e^{\mathcal{L}}$ increases more slowly than $S_e^{\mathcal{G}}$ and, thus, a Laplacian process is more fragile than the corresponding Gaussian process using the Fluctuation Theorem (16, 19, 20). In short, the fat tail phenomenon used to model market returns attempts to account for an increase in market risk due to market fragility. Because we have seen that $\Delta \text{Ric} \times \Delta S_e \geq 0$ (Ricci curvature is positively correlated with entropy), Ricci curvature seems to be a suitable and unexplored proxy to analyze systemic risk to date. Finally, we note that the above distributions are rarely used in practice as opposed to other distributions

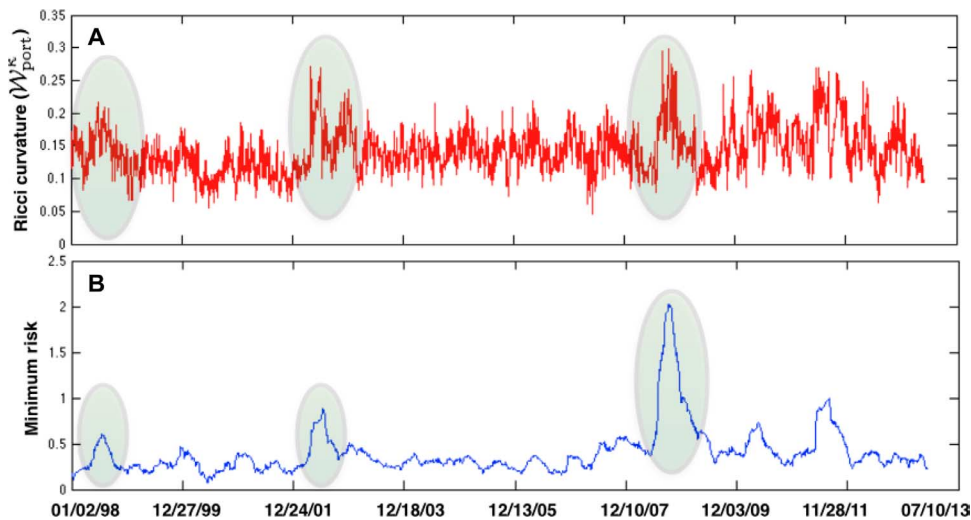


Fig. 6. Minimum risk Markowitz portfolio and Ricci curvature. We compute $W_{\text{port}}^{\mathcal{K}}$ using weights from the minimum risk portfolio along with minimum risk. (A and B) Regions of interest are highlighted for Ricci curvature $W_{\text{port}}^{\mathcal{K}}$ (A) and minimum risk (B) that can be obtained along the efficient frontier over a given window $T = 122$ days with a threshold of $\xi = 0.85$.

(for example, Student's t distribution) and are solely presented to motivate some of the concepts of the present work.

DISCUSSION

Given the 2007–2008 financial crisis and the current European debt crisis, it has become imperative to greatly improve our understanding of the fragility of interconnected networks. This work introduces a new geometric or economic indicator for systemic risk that captures local to global system-level fragility not only in financial markets but also for broader economic networks that include the banking ecosystem. There are a number of nontrivial facts that arise that may provide an understanding of commonly accepted financial models and, in turn, may uncover novel methodologies to account for systemic risk. The examples shown in this work illustrate the financial stock market, portfolio optimization, and heavy-tailed distributions in the geometric context of curvature. Moreover, although we provided an analysis in the context of stock correlation networks to elucidate market fragility, there seems to be interesting connections of Ricci curvature not only to the financial stability of various networks but also to the construction of market neutral strategies and possibly novel risk management policies. For example, previous work has noted that Ricci curvature is positively correlated with the mean-reversion coefficient in an Ornstein-Uhlenbeck process, which is a well-known family of stochastic processes that has been the basis for statistical arbitrage strategies (45). In short, this work makes the first mention of connecting the broad concept of curvature and statistical arbitrage and provides an interesting research direction that has not been previously explored.

There are several limitations in the present study that can be the subject of future research. In particular, although the data obtained represent stock correlation networks, it would be far more interesting to investigate specific banking environments for which derivative exposure has been argued to create instabilities (14). Understanding such types of risks will undoubtedly assist in one's understanding of some of the critical aspects of the 2007–2008 financial crisis. From a theoretical standpoint, the current methodology is for undirected networks; future research will seek to extend the present work toward directed graphs or networks. Furthermore, one can define geometric flows, such as the Ricci flow (that is, $\frac{d}{dt}d(x, y) = -\kappa(x, y)d(x, y)$), to combat and prevent financial contagions; this has been suggested in related fields (49) to remove overload queues in wireless networks. From a financial perspective, this is a particularly exciting research area because it may allow the FED to develop a set of quantitative nonsubjective policies that regulate financial risk exposure and provide an economic lending guide to provide emergency loans (that is, emergency funds to those institutions in a crisis period to decrease instability, as opposed to a "shotgun" lending approach).

In summary, our future work will seek to establish such policies that allow the market to be more cancer-like (more robust) (15), by providing novel "drug targets" to contain financial contagions, such as the 2007–2008 crisis that nearly brought down the financial system.

MATERIALS AND METHODS

Details on Ricci curvature

This section attempts to introduce some formal details on Ricci curvature (29) [see the book of do Carmo (8) for all the rigorous math-

ematical details]. Let X be a Riemannian manifold (the generalization of a smooth surface valid in any dimension). One can measure distances on X and, thus, define the length of a given curve γ . Geodesics are curves that, locally, have the shortest distance between two given points on the manifold X . Locally, such curves exist and will be critical to introducing the concept of curvature.

Next, given a point $x \in X$, let T_x denote the tangent space at x , and let $u_x, w \in T_x$ be orthogonal unit vectors. Then, if we traverse the manifold along the geodesic curve γ at x in the direction of w , we denote the endpoint of the traversal by $y \in X$. A pictorial representation of this is given in fig. S4. There exists a set of tangent vectors at y ; however, we are only interested in the specific tangent vector, denoted by $u_y \in T_y$, which would be the "same" as u_x ; that is, we want to compare two tangent vectors that live in different vector spaces in a canonical manner. This is done through parallel transport [see the book of do Carmo (8) for details about this operation]. Here, we simply state that u_y is the parallel transport of u_x .

Because of curvature, geodesics along u_x and u_y (denoted by $\exp_x tu_x$ and $\exp_y tu_y$, respectively; here, t denotes the curve parameter) may converge toward one another or diverge from one another (see fig. S5). With this in mind, we are able to define Ricci curvature through sectional curvature (8, 29). Again, for u_y , which is the parallel transport of $u = u_x$ from point x to point y in the direction w , we have, for sufficiently small $\epsilon, \delta > 0$

$$d(\exp_x \epsilon u_x, \exp_y \epsilon u_y) = \delta \left(1 - \frac{\epsilon^2}{2} K(u, w) + O(\epsilon^3 + \epsilon^2 \delta) \right) \quad (10)$$

The term $K(u, w)$ denotes the sectional curvature at x in the tangent plane (u, w) . Together, Ricci curvature is then simply obtained by averaging $K(u, w)$ over all directions u .

Details on Wasserstein distance

We next record the basic definition of the L^p Wasserstein distance (46) from optimal transport theory. The L^p Wasserstein distance is defined as

$$W_p(\mu_1, \mu_2) := \left(\inf_{\mu \in \Pi(\mu_1, \mu_2)} \iint d(x, y)^p d\mu(x, y) \right)^{1/p} \quad (11)$$

where X is a metric measure space equipped with distance d and $\Pi(\mu_1, \mu_2)$ is a set of all couplings between the measures μ_1 and μ_2 , which are assumed to have the same total mass and finite p th moments. More precisely, a coupling between μ_1 and μ_2 is a measure μ on $X \times X$, such that

$$\int_y d\mu(x, y) = d\mu_1(x), \int_x d\mu(x, y) = d\mu_2(y)$$

In other words, the marginals of μ are μ_1 and μ_2 . In this paper, we only considered the cases $p = 1, 2$. For completeness, we also define the Wasserstein distance (28) on discrete metric measure space $X = \{x_1, \dots, x_n\}$. Let μ_1 and μ_2 denote two distributions having the same total mass, and let $d(x, y)$ be the distance between $x, y \in X$ (for

Downloaded from <http://advances.sciencemag.org/> on November 18, 2017

graphs, taken as the hop metric). Then, $W_1(\mu_1, \mu_2)$ may be defined as follows (39)

$$W_1(\mu_1, \mu_2) = \min_{\mu} \sum_{i,j=1}^n d(x_i, x_j) \mu(x_i, x_j) \quad (12)$$

where $\mu(x, y)$ is a coupling (that is, distribution on $X \times X$) subject to the following constraints

$$\begin{aligned} \mu(x, y) &\geq 0 \text{ for } x, y \in X \\ \sum_{i=1}^n \mu(x, x_i) &= \mu_1(x) \text{ for } x \in X \\ \sum_{i=1}^n \mu(x_i, y) &= \mu_2(y) \text{ for } y \in X \end{aligned}$$

The cost above finds the optimal coupling of moving mass defined by the distributions μ_1 to μ_2 with minimal “work.” Clearly, the optimal coupling μ may be found using linear programming [see the work of Evans (32)].

Details on network entropy

This section provides some key facts about network entropy. Accordingly, consider a stochastic matrix $\phi = (\eta_{xy})$ describing a Markov chain that characterizes transition rates from state x to state y with $\eta_{xy} \geq 0$ and $\sum_y \eta_{xy} = 1$ (along with its invariant distribution $\pi = \pi\phi$). Then, network entropy may be defined as

$$S_e = \sum_x \pi(x) \bar{S}(x) \text{ with } \bar{S}(x) = -\sum_y \eta_{xy} \log \eta_{xy} \quad (13)$$

We note that in the above definition, the nodal entropy $S(x)$ is the summation only over edges y adjacent to x . This is particularly important because it discounts information from nonadjacent vertices. Note that the computation for n -step random walks (Markov processes) with $n > 1$ may become computationally expensive (50). Thus, accounting for indirect complex effects becomes computationally burdensome. As we have seen, Ollivier-Ricci curvature can be formulated as a simple linear program and is not restricted to direct incidences. Also, local (nodal) entropy “loses information” with respect to edge information through a weighted contraction; this quantification of edge fragility is precisely what Ricci curvature provides. These two important caveats motivate our proposal for the use of curvature over entropy as a proxy for system-level fragility.

SUPPLEMENTARY MATERIALS

Supplementary material for this article is available at <http://advances.sciencemag.org/cgi/content/full/2/5/e1501495/DC1>

- fig. S1. Example of setting up the problem.
- fig. S2. Illustration of transporting regions on nonnegatively curved space.
- fig. S3. Illustration of how shortest path relates to curvature or entropy.
- fig. S4. Intuitive understanding of Ricci curvature (a different perspective).
- fig. S5. Illustrating geodesic deviations on nonnegatively curved space.

REFERENCES AND NOTES

1. F. Schweitzer, G. Fagiolo, D. Sornette, F. Vega-Redondo, A. Vespignani, D. R. White, Economic networks: The new challenges. *Science* **325**, 422–425 (2009).
2. S. Battiston, M. Puliga, R. Kaushik, P. Tasca, G. Caldarelli, DebtRank: Too central to fail? Financial networks, the FED and systemic risk. *Sci. Rep.* **2**, 541 (2012).

3. A. G. Haldane, R. M. May, Systemic risk in banking ecosystems. *Nature* **469**, 351–355 (2011).
4. R. N. Mantegna, Hierarchical structure in financial markets. *Eur. Phys. J. B* **11**, 193–197 (1999).
5. J.-P. Onnela, A. Chakraborti, K. Kaski, J. Kertész, A. Kanto, Dynamics of market correlations: Taxonomy and portfolio analysis. *Phys. Rev. E Stat. Nonlin. Soft Matter Phys.* **68**, 056110 (2003).
6. M. Bardoscia, S. Battiston, F. Caccioli, G. Caldarelli, DebtRank: A microscopic foundation for shock propagation. *PLOS One* **10**, e0130406 (2015).
7. U.S. Government Accountability Office (GAO), “Opportunities exist to strengthen policies and processes for managing emergency assistance” (Technical Report GAO-11-696, 2011); www.gao.gov/products/GAO-11-696.
8. M. P. do Carmo, *Riemannian Geometry* (Birkhäuser, Boston, MA, 1992), 300 pp.
9. Y. Ollivier, Ricci curvature of Markov chains on metric spaces. *J. Funct. Anal.* **256**, 810–864 (2009).
10. Y. Ollivier, Ricci curvature of metric spaces. *C. R. Math.* **345**, 643–646 (2007).
11. J. Lott, C. Villani, Ricci curvature for metric-measure spaces via optimal transport. *Ann. Math.* **169**, 903–991 (2009).
12. J. Maas, Gradient flows of the entropy for finite Markov chains. *J. Funct. Anal.* **261**, 2250–2292 (2011).
13. S.-N. Chow, W. Huang, Y. Li, H. Zhou, Fokker–Planck equations for a free energy functional or Markov process on a graph. *Arch. Ration. Mech. Anal.* **203**, 969–1008 (2012).
14. S. Battiston, G. Caldarelli, C.-P. Georg, R. May, J. Stiglitz, Complex derivatives. *Nat. Phys.* **9**, 123–125 (2013).
15. R. Sandhu, T. Georgiou, E. Reznik, L. Zhu, I. Kolesov, Y. Senbabaoglu, A. Tannenbaum, Graph curvature for differentiating cancer networks. *Sci. Rep.* **5**, 12323 (2015).
16. L. Demetrius, T. Manke, Robustness and network evolution—An entropic principle. *Phys. A* **346**, 682–696 (2005).
17. R. Albert, A.-L. Barabási, Statistical mechanics of complex networks. *Rev. Mod. Phys.* **74**, 47 (2002).
18. A.-L. Barabási, The network takeover. *Nat. Phys.* **8**, 14–16 (2012).
19. L. A. Demetrius, Boltzmann, Darwin, and directionality theory. *Phys. Rep.* **530**, 1–85 (2013).
20. L. Demetrius, V. M. Gundlach, G. Ochs, Complexity and demographic stability in population models. *Theor. Popul. Biol.* **65**, 211–225 (2004).
21. S. Battiston, D. Delli Gatti, M. Gallegati, B. Greenwald, J. E. Stiglitz, Liaisons dangereuses: Increasing connectivity, risk sharing, and systemic risk. *J. Econ. Dyn. Control* **36**, 1121–1141 (2012).
22. M. Elliot, B. Golub, M. O. Jackson, Financial networks and contagion. *Am. Econ. Rev.* **104**, 3115–3153 (2014).
23. F. Allen, D. Gale, Financial contagion. *J. Polit. Econ.* **108**, 1–33 (2000).
24. S. Vitali, J. B. Glattfelder, S. Battiston, The network of global corporate control. *PLOS One* **6**, e25995 (2011).
25. J.-P. Onnela, A. Chakraborti, K. Kaski, J. Kertész, Dynamic asset trees and portfolio analysis. *Eur. Phys. J. B* **30**, 285–288 (2002).
26. J.-P. Onnela, A. Chakraborti, K. Kaski, J. Kertész, Dynamic asset trees and Black Monday. *Phys. A* **324**, 247–252 (2003).
27. H. Markowitz, Portfolio selection. *J. Finance* **7**, 77–91 (1952).
28. Y. Rubner, C. Tomasi, L. J. Guibas, The Earth Mover’s Distance as a metric for image retrieval. *Int. J. Comput. Vision* **40**, 99–121 (2000).
29. Y. Ollivier, A visual introduction to Riemannian curvatures and some discrete generalizations, in *Analysis and Geometry of Metric Measure Spaces: Lecture Notes of the 50th Séminaire de Mathématiques Supérieures (SMS), Montréal, 2011* (American Mathematical Society, Washington, DC, 2013), pp. 197–219.
30. C. Villani, *Optimal Transport: Old and New* (Springer-Verlag, Berlin, Germany, 2008), 976 pp.
31. C. Villani, *Topics in Optimal Transportation* (American Mathematical Society, Washington, DC, 2003), 370 pp.
32. L. C. Evans, Partial differential equations and Monge–Kantorovich mass transfer, in *Current Developments in Mathematics* (International Press, Boston, MA, 1999), pp. 65–126.
33. E. Tannenbaum, T. Georgiou, A. Tannenbaum, Signals and control aspects of optimal mass transport and the Boltzmann entropy, paper presented at the 49th Institute of Electrical and Electronics Engineers Conference on Decision and Control (CDC), Atlanta, GA, 15 to 17 December 2010.
34. C. R. Givens, R. M. Shortt, A class of Wasserstein metrics for probability distributions. *Mich. Math. J.* **31**, 231–240 (1984).
35. A.-I. Bonciocat, K.-T. Sturm, Mass transportation and rough curvature bounds for discrete spaces. *J. Funct. Anal.* **256**, 2944–2966 (2009).
36. R. J. McCann, A convexity principle for interacting gases. *Adv. Math.* **128**, 153–179 (1997).
37. K.-T. Sturm, Probability measures on metric spaces of nonpositive curvature. *Contemp. Math.* **338**, 1–34 (2003).

38. M. Gromov, Hyperbolic groups, in *Essays in Group Theory*, vol. 8 of *Mathematical Sciences Research Institute Publications* (Springer, New York, 1987), pp. 75–263.
39. M. Puliga, G. Caldarelli, S. Battiston, Credit default swaps networks and systemic risk. *Sci. Rep.* **4**, 6822 (2014).
40. V. Boginski, S. Butenko, P. M. Pardalos, Mining market data: A network approach. *Comput. Oper. Res.* **33**, 3171–3184 (2006).
41. C. K. Tse, J. Liu, F. C. M. Lau, A network perspective of the stock market. *J. Empir. Financ.* **17**, 659–667 (2010).
42. F. Bauer, J. Jost, S. Liu, Ollivier-Ricci curvature and the spectrum of the normalized graph Laplace operator. (2001). <http://arxiv.org/abs/1105.3803>.
43. T. Preis, D. Y. Kenet, H. E. Stanley, D. Helbing, E. Ben-Jacob, Quantifying the behavior of stock correlations under market stress. *Sci. Rep.* **2**, 752 (2012).
44. M. Kritzman, Y. Li, Skulls, financial turbulence, and risk management. *Financ. Anal. J.* **66**, 30–41 (2010).
45. A. D'Apsremont, Identifying small mean-reverting portfolios. *Quant. Financ.* **11**, 351–364 (2011).
46. S. Rachev, L. Ruschendorf, *Mass Transportation Problems, Vol. I and II* (Springer-Verlag, New York, 1998), 430 pp.
47. S. Rachev, *Handbook of Heavy Tailed Distributions in Finance: Handbooks in Finance* (Elsevier, Amsterdam, Netherlands, 2003), 704 pp.
48. B. B. Mandelbrot, *Fractals and Scaling in Finance: Discontinuity, Concentration, Risk* (Springer, New York, 1997), 552 pp.
49. C. Wang, E. Jonckheere, R. Bainrazi, Wireless network capacity versus Ollivier-Ricci curvature under heat diffusion protocol, paper presented at the Institute of Electrical and Electronics Engineers American Control Conference, Portland, OR, 4 to 6 June 2014.
50. J. West, G. Bianconi, S. Severini, A. E. Teschendorff, Differential network entropy reveals cancer system hallmarks. *Sci. Rep.* **2**, 802 (2012).

Acknowledgments

Funding: This work was supported by the U.S. Air Force Office of Scientific Research grants FA9550-12-1-0319 and FA9550-15-1-0045. **Author contributions:** R.S.S., T.T.G., and A.R.T. developed the mathematical framework and the necessary code and analysis used in this work. **Competing interests:** The authors declare that they have no competing interests. **Data and materials availability:** All data needed to evaluate the conclusions in the paper are available at <http://quantquote.com> or are present in the paper and/or the Supplementary Materials. Additional data related to this paper may be requested from the authors.

Submitted 21 October 2015

Accepted 22 April 2016

Published 27 May 2016

10.1126/sciadv.1501495

Citation: R. S. Sandhu, T. T. Georgiou, A. R. Tannenbaum, Ricci curvature: An economic indicator for market fragility and systemic risk. *Sci. Adv.* **2**, e1501495 (2016).

Ricci curvature: An economic indicator for market fragility and systemic risk

Romeil S. Sandhu, Tryphon T. Georgiou and Allen R. Tannenbaum

Sci Adv 2 (5), e1501495.

DOI: 10.1126/sciadv.1501495

ARTICLE TOOLS

<http://advances.sciencemag.org/content/2/5/e1501495>

SUPPLEMENTARY MATERIALS

<http://advances.sciencemag.org/content/suppl/2016/05/24/2.5.e1501495.DC1>

REFERENCES

This article cites 37 articles, 1 of which you can access for free
<http://advances.sciencemag.org/content/2/5/e1501495#BIBL>

PERMISSIONS

<http://www.sciencemag.org/help/reprints-and-permissions>

Use of this article is subject to the [Terms of Service](#)

Science Advances (ISSN 2375-2548) is published by the American Association for the Advancement of Science, 1200 New York Avenue NW, Washington, DC 20005. 2017 © The Authors, some rights reserved; exclusive licensee American Association for the Advancement of Science. No claim to original U.S. Government Works. The title *Science Advances* is a registered trademark of AAAS.